

# Dynamic Breakdown Characteristics of Liquid Helium Induced by a Quench of Superconducting Wire and Coil

H. Okubo, M. Wakita, S. Chigusa,

Department of Electrical Engineering, Nagoya University, Japan

N. Hayakawa

Center for Integrated Research in Science  
and Engineering, Nagoya University

and M. Hikita

Department of Electrical Engineering, Kyushu Institute of Technology, Japan

## ABSTRACT

For practical insulation design of superconducting power apparatus, it is necessary to take into account an inherent phenomenon known as quench. The transition from the superconducting to the normal state. We investigated quench-induced dynamic breakdown and prebreakdown characteristics of liquid helium (LHe). Experimental results revealed that the quench of the superconductor drastically reduced the breakdown voltage of LHe in the thermal bubble disturbance. Moreover, dynamic breakdown characteristics in quasi-uniform field using superconducting coil were investigated. The results revealed that the breakdown was induced in the quench-initiated region where the largest thermal energy was generated.

## 1. INTRODUCTION

As superconducting electric power systems tend to be operated under HV environment, electrical insulation technology at cryogenic temperatures is getting more important [1-4]. Many papers on HV breakdown characteristics in cryogenic liquids have been reported, however most of investigations have been so far limited only on fundamental or 'static' breakdown characteristics of cryogenic liquids [5-9]. Thus, it is necessary to evaluate the insulation performance of cryogenic liquids under practical operating conditions of power apparatus.

It is well known that superconducting power apparatus have an inherent phenomenon called 'quench': the transition from superconducting to the normal state. The quench phenomenon causes the generation and the propagation of voltage and ohmic heat in cryogenic liquids out of superconducting wires or coils [10]. Under high electric field, the quench would greatly affect the electrical insulation performance of cryogenic liquids and we call this phenomenon quench-induced 'dynamic' breakdown characteristics, different from the static ones. The dynamic breakdown characteristics are regarded

as one of the phenomena peculiar to the superconducting/cryogenic environment.

From the above viewpoints, we have investigated the dynamic breakdown characteristics of liquid helium (LHe) induced by a quench of superconducting wires [11-12]. In the present paper, we first discuss the influence of thermal bubble behavior due to quench induced dynamic breakdown characteristics.

Secondly, we describe the effect of electric field distribution on dynamic breakdown. Moreover, measurement results of dynamic breakdown induced by quench of superconducting coil were described. We also made clear the relationship between the dynamic breakdown of LHe and the generation and propagation of quench of superconducting coil.

## 2. EXPERIMENTAL

Figure 1 shows the experimental setup for the measurement of static and dynamic breakdown characteristics of LHe [12]. This circuit consists of a HV source including a plane electrode and a large current source including a superconducting coil. The plane electrode

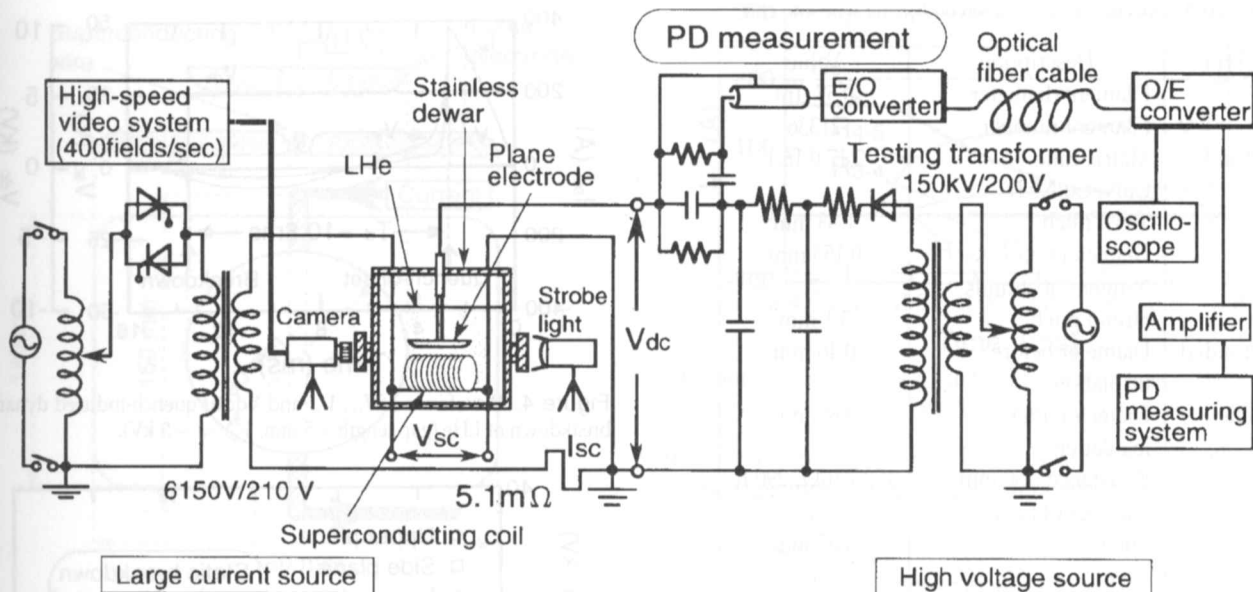


Figure 1. Experimental setup for measuring static and dynamic breakdown characteristics of LHe.

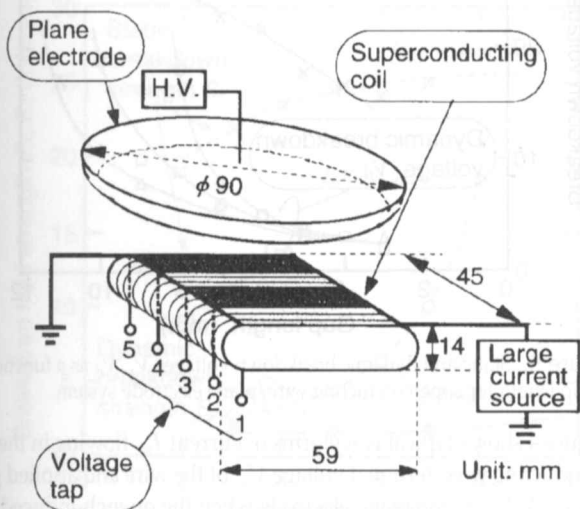


Figure 2. Electrode configuration for superconducting coil/plane electrode system.

was placed in parallel above the superconducting coil and they were immersed in saturated LHe with atmospheric pressure at 4.2 K. Figure 2 shows the electrode configuration for superconducting coil/plane electrode system. The plane electrode was made of stainless steel, the surface of which was polished to a mirror finish. The superconducting coil had a flat shape to make the electric field quasi-uniform in the gap space, so that we can investigate the effect of quench propagation on dynamic breakdown of LHe. Five voltage taps were arranged out of the superconducting coil at regular intervals to analyze the quench propagation in the coil. We also investigate the fundamental aspects of quench-induced dynamic breakdown characteristics of LHe under uniform and non-uniform electric fields by replacing the superconducting coil in Figure 2 with superconducting short wire as will be shown later in Figures 3 and 6. Table 1 summarizes the specifications of the superconducting wire and coil used in

the experiments. The stranded cable for short wire experiment had no wire-insulation, on the other hand, the cable for superconducting coil had the insulation layer of epoxy resin for turn insulation. The insulation layer has never been damaged in course of helium breakdown. We confirmed the sufficient insulation performance at the final stage of the experiment. Dimensions of the superconducting coil are also shown in Figure 2. The gap length  $g$  between the plane electrode and the coil can be adjusted from  $g = 0$  to  $\sim 10$  mm.

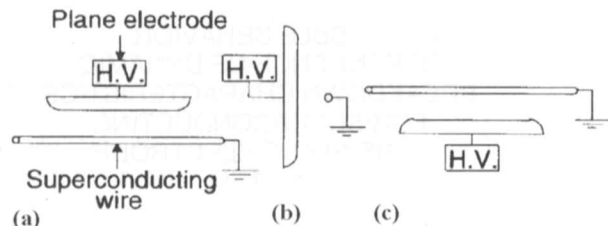


Figure 3. Arrangement of superconducting wire/plane electrode configuration. (a) Upper plane, (b) side plane, (c) lower plane.

HV dc was applied to the plane electrode and kept at a constant value below the static breakdown level. In this condition, quench was induced by large current flowing in the superconducting coil during 1 cycle of 60 Hz. Owing to the quench, thermal bubbles were generated out of superconducting coil and induced dynamic breakdown of LHe. We measured three transient waveforms with a digital storage oscilloscope (100 MHz): the current  $I_{sc}$  flowing in the superconducting coil, the induced voltage  $V_{sc}$  across the superconducting coil and the applied dc voltage  $V_{dc}$  before and after quench. At the same time, we observed the generation and the propagation of bubbles in the gap space through a high-speed video system (400 fields/s). Partial discharges (PD) characteristics were also measured with 10 pC sensitivity during the process from quench-onset to dynamic breakdown.

Table 1. Specifications of superconducting wire and coil.

Type	Description	Value
Strand	Filament diameter	0.57 $\mu\text{m}$
	Filament number	21336
	Matrix ratio	2.17:0.16:1
	CuNi:Cu:NbTi	
	Twist pitch	1.33 mm
	Diameter	0.153 mm
Stranded cable	Number of strands	7
	Strand pitch	3.1 mm
	Diameter before insulation	0.46 mm
	Diameter after insulation	0.67 mm
	Resistance, 150 mm	152.7 m $\Omega$ , 290 K
Coil	Number of turns	62
	Pitch	0.67 mm
	Layer	1
	Wire length	8.9 m
	Resistance	8.45 $\Omega$ , 290 K
	Self inductance	71 $\mu\text{H}$

### 3. RESULTS AND DISCUSSIONS

#### 3.1. FUNDAMENTAL CHARACTERISTICS OF DYNAMIC BREAKDOWN FOR SINGLE SUPERCONDUCTING WIRE/PLANE ELECTRODE SYSTEM.

##### 3.1.1. BUBBLE BEHAVIOR DEPENDENCE OF DYNAMIC BREAKDOWN CHARACTERISTICS FOR SUPERCONDUCTING WIRE/PLANE ELECTRODE SYSTEM.

Figure 3 shows the three different arrangements of superconducting wire/plane electrode configuration. As shown in this Figure, we call each configuration as (a) upper plane, (b) side plane and (c) lower plane, respectively. All of these electrode configurations give us non-uniform electric field distribution.

We have already investigated fundamental characteristics of quench-induced dynamic breakdown of LHe under non-uniform electric field distribution for Upper plane configuration [11–13]. Under such a non-uniform field, thermal bubble behavior in the vicinity of the superconducting wire is dominated by the gradient force rather than buoyancy and viscous force [12]. However, the gradient force is drastically attenuated with approaching to the plane electrode where the electric field is quite low, and the buoyancy becomes dominant. Thus, the bubble behavior depends on the relative direction of the gradient force and the buoyancy, affecting the dynamic breakdown of LHe. The above three electrode configurations shown in Figure 3 allow the bubble behavior to drive different direction.

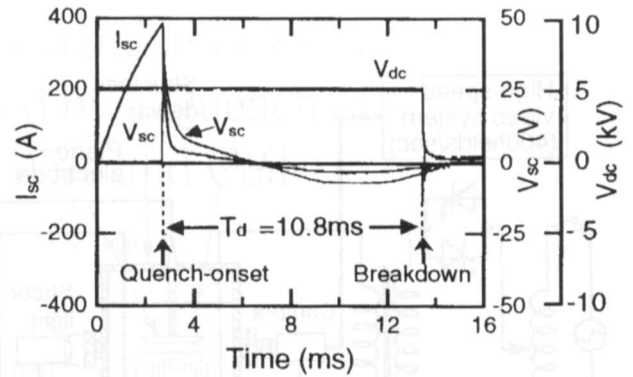


Figure 4. Waveforms of  $I_{sc}$ ,  $V_{sc}$  and  $V_{dc}$  at quench-induced dynamic breakdown of LHe (gap length = 5 mm,  $V_{dc} = +5$  kV).

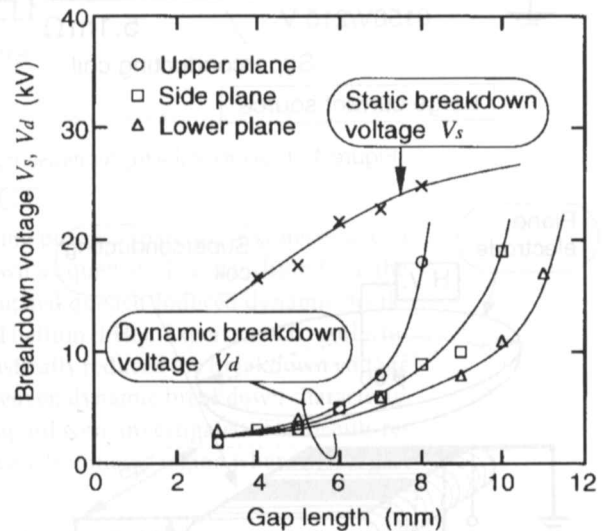


Figure 5. Static and dynamic breakdown voltages  $V_s$ ,  $V_d$  as a function of gap length for superconducting wire/plane electrode system.

Figure 4 shows typical waveforms of current  $I_{sc}$  flowing in the superconducting wire, terminal voltage  $V_{sc}$  of the wire and applied positive dc HV  $V_{dc}$  to the plane electrode when the quench-induced dynamic breakdown occurred for Upper plane electrode configuration with  $g = 5$  mm and  $V_{dc} = +5$  kV. The quench of superconducting wire occurred at the current value of 380 A, and at the instance, the terminal voltage  $V_{sc}$  of superconducting wire suddenly rose. Dynamic breakdown was induced at 10.8 ms after the quench-onset, depending on the bubble propagation.

Figure 5 shows obtained gap length dependence of dynamic breakdown voltage of LHe, as well as the static one. The static breakdown voltage  $V_s$  was measured by applying a positive dc ramp voltage at a rate of 1 kV/s without current flowing in the superconducting wire. Let us define dynamic breakdown voltage  $V_d$  as the minimum value of applied voltage below which the breakdown is no longer induced by the quench at each gap length. As shown in Figure 5,  $V_d$  is much smaller than  $V_s$  for a given gap length.  $V_d$  is independent of the electrode configurations for  $g < 6$  mm, while it depends on the electrode configurations with enlarging the gap length.

At the small gap length, the dynamic breakdown occurred when

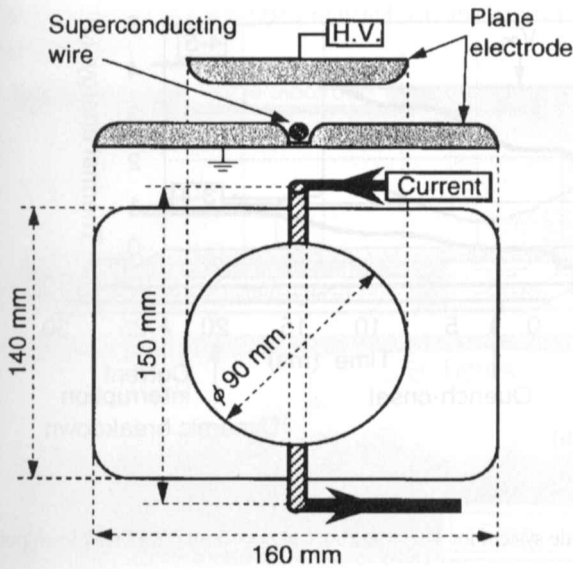


Figure 6. Electrode configuration for plane/plane with embedded superconducting wire.

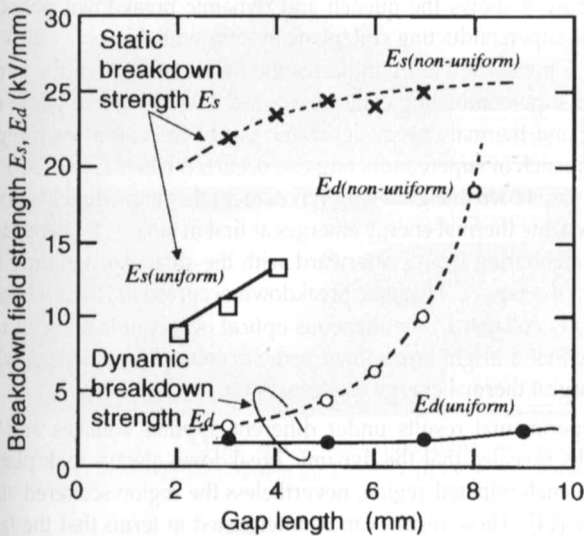


Figure 7. Static and dynamic breakdown field strengths  $E_s$ ,  $E_d$  as a function of gap length for superconducting wire/plane electrode system.

the front of thermal bubble cluster generated by the quench reached the plane electrode and bridged the gap space. For all electrode configurations in Figure 3, thermal bubbles propagate toward the plane electrode owing to the dominant gradient force irrespective of the relative direction to the buoyancy. Thus,  $V_d$  is considered to be independent of the electrode configurations.

On the other hand, at the large gap length, it is supposed that the dynamic breakdown took place in the disturbance where the gap space was filled with thermal bubbles generated continuously out of the superconducting wire and those rebounded from the plane electrode. For all electrode configurations used in this experiment, the dynamic breakdown was confirmed to occur in the thermal bubble disturbance in the gap space. Especially, in the case of lower plane, thermal bubbles rebounded from the plane electrode propagate in the same direction as buoyancy, so that bubble density in the gap space

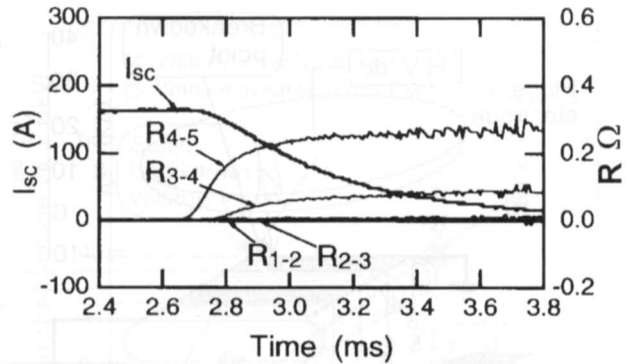


Figure 8. Waveforms of  $I_{sc}$  and resistance in each region between taps before and after quench of superconducting coil.

around the wire, in particular, becomes larger than the other arrangements. Therefore,  $V_d$  is the smallest for lower plane electrode configuration. In the case of Side plane, since bubbles rebounded downward contribute to the enlargement of disturbance,  $V_d$  lied between those for Upper plane and for lower plane.

### 3.1.2. EFFECT OF ELECTRIC FIELD DISTRIBUTION ON DYNAMIC BREAKDOWN FOR SUPERCONDUCTING WIRE/PLANE ELECTRODE SYSTEM.

In the previous subsection, we discussed the dynamic breakdown characteristics of LHe under non-uniform electric field distribution, using a single superconducting wire/plane electrode system. In this subsection, we measure the dynamic breakdown characteristics under uniform field for superconducting wire/plane electrode system so as to discuss the influence of electric field distribution on the breakdown. Figure 6 shows the electrode configuration to make the electric field uniform in the gap space. To make a uniform field, another plane electrode with a groove for superconducting wire was placed under the plane electrode; macroscopic electric field was made uniform between two plane electrodes.

Figure 7 shows the gap length dependence of static and dynamic breakdown field strengths of LHe under uniform electric field for positive dc voltage application to the upper plane electrode. This Figure also represents the breakdown characteristics under non-uniform field for Upper plane electrode configuration shown in Figure 5. Note that in non-uniform field, dynamic breakdown field strength was defined as that on the surface of the superconducting wire at the breakdown.

As shown in this Figure, dynamic breakdown field strength  $E_{d(u)}$  and  $E_{d(n)}$  under both uniform and non-uniform fields are much smaller than static breakdown strength  $E_{s(u)}$  and  $E_{s(n)}$ , respectively.  $E_{d(n)}$  increases exponentially with increasing gap length, while  $E_{d(u)}$  is almost independent of gap length with a constant value  $\sim 2$  kV/mm.  $E_{d(u)}$  is found to be smaller than  $E_{d(n)}$ . In the process from quench-onset to dynamic breakdown, PD was detected under the non-uniform field but no PD was detected under uniform field.

These results suggest that dynamic breakdown under the uniform

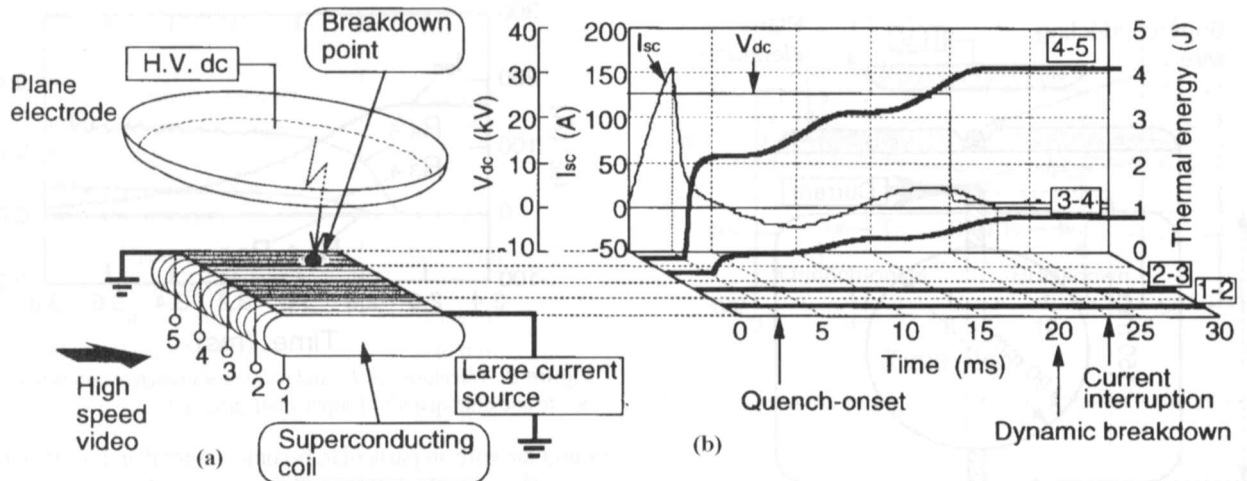


Figure 9. Quench and dynamic breakdown for superconducting coil-plane electrode system for  $V_{dc} = +25$  kV at  $g = 5$  mm. (a) Breakdown point. (b) Time evolution of  $I_{sc}$ ,  $V_{dc}$  and thermal energy.

field is determined by discharge inception in thermal bubbles. In other words, under the uniform field, breakdown bridging over the gap space occurs as soon as discharge takes place locally in the thermal bubbles because of uniform and high field stress in the gap space. On the other hand, under the non-uniform field, PD are followed by dynamic breakdown of LHe in the bubbles exposed to extremely high electric field in the vicinity of superconducting wire [13]. Thus, when the electric field stress on the surface of the superconducting wire lies between  $E_{d(u)}$  and  $E_{d(n)}$ , PD occur, but do not result in the dynamic breakdown. Consequently,  $E_{d(n)}$  is considered to be larger than  $E_{d(u)}$ .

### 3.2. DYNAMIC BREAKDOWN AND QUENCH PROPAGATION BY SUPERCONDUCTING COIL.

In order to investigate further practical insulation performance of superconducting power apparatus, a coil configuration should be taken into consideration. This Section deals with the quench-induced dynamic breakdown characteristics for superconducting coil/plane electrode system shown in Figure 2. Quench of the superconducting coil propagates 2-dimensionally on the coil surface along the wire under quasi-uniform electric field.

Voltage taps arranged on the superconducting coil enable us to analyze the quench propagation characteristics in the coil. Voltage signal between taps is composed of the resistive component due to quench and inductive component by self-inductance of the coil. We can pick up only the resistive component through signal processing technique, resulting in finding the quench-initiated region. Figure 8 shows time variations of the resistance due to quench in each region divided by voltage taps. The horizontal axis in Figure 8 represents time from the inception of current flowing in the coil. Resistance is firstly observed at 2.65 ms in the region between tap 4 and 5 (tap<sub>4-5</sub>, hereinafter) and then, current  $I_{sc}$  gradually decreases. After that, resistance also appears in tap<sub>3-4</sub> at 2.75 ms. The result means that the quench was initiated in tap<sub>4-5</sub> and propagated into tap<sub>3-4</sub>. As shown in Figure 8,

we can detect the quench-initiated region in the superconducting coil.

Figure 9 shows the quench and dynamic breakdown phenomena for superconducting coil/plane system with  $V_{dc} = +25$  kV at  $g = 5$  mm. The Figure indicates the time evolution of the current  $I_{sc}$  of superconducting coil, the applied HV  $V_{dc}$  to the plane electrode and thermal energy generated out of the coil in each region. The quench of superconducting coil occurred when  $I_{sc} = 155$  A at 2.5 ms as shown in Figure 9(b). It is evident that immediately after the quench, the thermal energy emerges at first in tap<sub>4-5</sub>, and appears in the neighboring tap<sub>3-4</sub> afterward with the smaller magnitude than that in the tap<sub>4-5</sub>. Dynamic breakdown occurred at 20 ms when  $V_{dc}$  abruptly collapsed. Simultaneous optical observation allowed us to verify that a bright breakdown path was observed in tap<sub>4-5</sub> where the largest thermal energy was generated.

Experimental results under different applied voltages and gap lengths revealed that the dynamic breakdown always took place in the quench-initiated region, nevertheless the region scattered statistically [14]. These results can be interpreted in terms that the larger thermal energy due to quench generates the larger disturbance by thermal bubbles in the gap space, resulting in the dynamic breakdown.

Figure 10 shows pictures of bubble behavior and dynamic breakdown with  $V_{dc} = +40$  kV at  $g = 8$  mm. In this case, quench and dynamic breakdown took place in tap<sub>3-4</sub> of the center region of the superconducting coil. As shown in the pictures, at 5 ms after quench-onset, thermal bubbles are generated near the center of the superconducting coil. Note that at 15 ms, the head of thermal bubble cluster reaches the plane electrode. Finally, the dynamic breakdown occurs in tap<sub>3-4</sub> in the bubble disturbance in the gap space at 102 ms.

Figure 11 shows the relationship between the quench-initiated region and dynamic breakdown location of LHe through the simultaneous observation of quench and dynamic breakdown. For example, when the quench was firstly initiated  $11\times$  in tap<sub>4-5</sub>, dynamic breakdown took place  $10\times$  in tap<sub>4-5</sub>, while only once in tap<sub>1-2</sub>. As shown in this Figure, it was clarified that dynamic breakdown occurred in the

region where the quench was firstly initiated with the largest thermal energy generation.

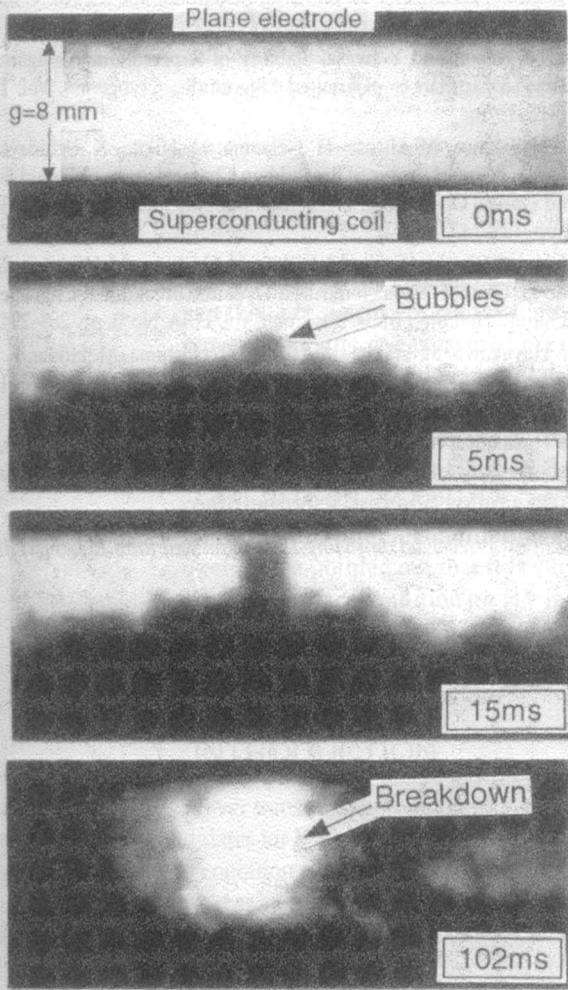


Figure 10. Bubble behavior and dynamic breakdown for superconducting coil/plane electrode system for  $V_{dc} = +40$  kV at  $g = 8$  mm.

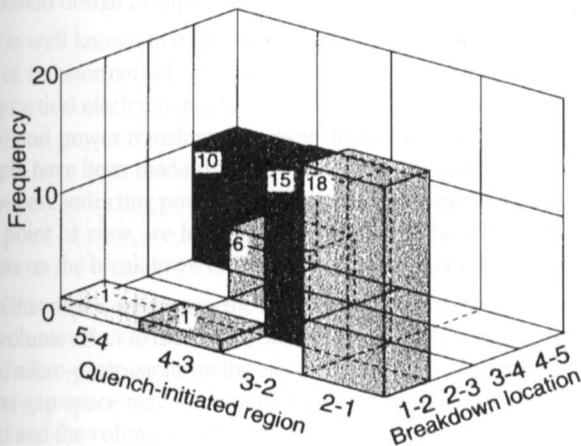


Figure 11. Relationship between quench-initiated region and dynamic breakdown location of LHe.

Figure 12 shows the gap length dependence of static and dynamic breakdown voltages of LHe for superconducting coil/plane system

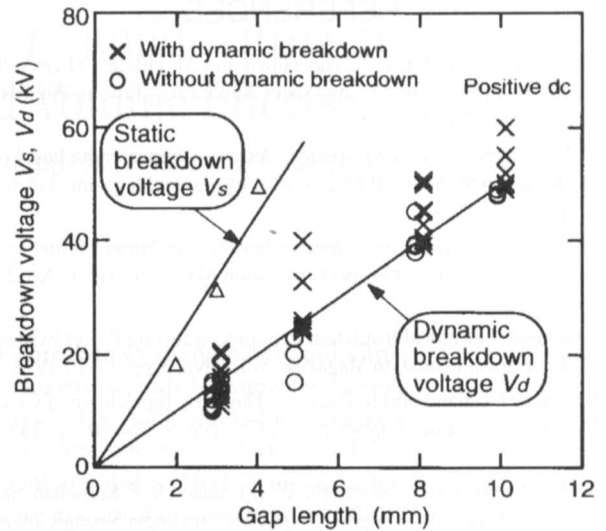


Figure 12. Static and dynamic breakdown voltage  $V_s, V_d$  as a function of gap length for superconducting coil/plane electrode system.

for a positive dc voltage application. As seen in this Figure,  $V_d$  also falls down against  $V_s$  as well as those for superconducting wire/plane system. At  $g = 3$  mm,  $V_d = +15$  kV and  $V_s = +32$  kV, that is, the quench reduces the breakdown voltage of LHe into 47% under quasi-uniform electric field. It is also seen that the dynamic breakdown field strength is evaluated as 5 kV/mm from the slope of the approximated line. From this result, future superconducting power apparatus are suggested to be designed under such a low breakdown strength with taking account of their quench environment.

#### 4. CONCLUSIONS

THIS paper presented the effect of both thermal bubble behavior due to quench and electric field distribution on quench-induced dynamic breakdown characteristics of LHe. Under both non-uniform and uniform electric fields, the quench of superconducting wire considerably could reduce breakdown voltage. Dynamic breakdown was induced by partial discharges associated with the bubble behavior under non-uniform field. On the other hand, it was verified that under uniform field, dynamic breakdown of LHe occurred as soon as discharge took place locally in the thermal bubbles without partial discharges.

Moreover, we investigated dynamic breakdown characteristics induced by quench of superconducting coil. For superconducting coil/plane system under quasi-uniform field, the quench-induced dynamic breakdown strength proved to be 5 kV/mm, and reduced into 47% compared with the static one. Simultaneous observation of quench propagation and dynamic breakdown path revealed that the dynamic breakdown took place in the quench-initiated region where the largest amount of bubbles were generated due to thermal energy after quench.

Consequently, the quench-induced dynamic breakdown characteristics should be taken into consideration to evaluate the practical insulation performance of LHe as a peculiar factor to superconducting/geniogenic environment.

## REFERENCES

- [1] H. Okubo, H. Goshima, N. Hayakawa and M. Hikita, "High Voltage Insulation of Superconducting Power Apparatus", Proc. of 9th ISH, Invited Lecture, No. 9007, 1995.
- [2] E. B. Forsyth, "The High Voltage Design of Superconducting Power Transmission Systems", IEEE Electrical Insulation Magazine, Vol. 6, No. 4, pp. 7-16, 1990.
- [3] H. Fujino, "Electrical Insulation Technology for Superconducting Devices in Japan", IEEE Electrical Insulation Magazine, Vol. 6, No. 2, pp. 7-15, 1990.
- [4] J. Gerhold, "Electrical Insulation in Superconducting Power Systems.", IEEE Electrical Insulation Magazine, Vol. 8, No. 3, pp. 14-20, 1992.
- [5] B. Fallou, J. Galand and B. Bouvier, "Dielectric Breakdown of Gaseous Helium at very Low Temperatures", Cryogenics, Vol. 10, pp. 142-145, 1970.
- [6] M. M. Menon, S. W. Schwenterly, W. F. Gauster, R. F. Kernohan and H. M. Long, "Dielectric Strength of Liquid Helium under Strongly Inhomogeneous Field Conditions", Advances in Cryogenic Engineering, Vol. 21, pp. 95-101, 1976.
- [7] J. Gerhold, "Breakdown Phenomena in Liquid Helium", IEEE Trans. on Electrical Insulation, Vol. 24, No. 2, pp. 155-166, 1989.
- [8] R. J. Meats, "Pressurized-helium Breakdown at very Low Temperatures", Proc of IEE, Vol. 119, No. 6, pp. 760-766, 1972.
- [9] M. Hara, T. Kaneko and K. Honda, "Thermal-bubble Initiated Breakdown Characteristics of Liquid Helium and Nitrogen at Atmospheric Pressure", IEEE Trans. on Electrical Insulation, Vol. 23, No. 4, pp. 769-778, 1988.
- [10] M. N. Wilson and Y. Iwasa, Stability of Superconductors against Localized Disturbances of Limited Magnitude., Cryogenics, Vol. 18, pp. 17-25, 1978.
- [11] N. Hayakawa, M. Hirose, H. Goshima, M. Hikita, K. Uchida and H. Okubo, "Quench-induced Breakdown Characteristics of Liquid Helium and Optical Observation of Thermal Bubbles", Cryogenics, Vol. 35, No. 2, pp. 135-142, 1995.
- [12] N. Hayakawa, M. Hirose, M. Wakita, H. Goshima, M. Hikita, K. Uchida and H. Okubo, "Quench-induced Dynamic Breakdown Characteristics of Liquid Helium", Trans. IEE Japan, Vol. 115A, No. 3, pp. 288-294, 1995.
- [13] N. Hayakawa, M. Wakita, M. Hirose, H. Goshima, M. Hikita, K. Uchida and H. Okubo, "Quench-induced Breakdown Mechanism of Liquid Helium", Proc. of 9th ISH, No. 7047, 1995.
- [14] N. Hayakawa, M. Wakita, H. Goshima, M. Hikita and H. Okubo, "Statistical Analysis of Scattering in Quench Current of ac Superconducting Wires", ICEC 16/ICMC, PS2-m1-22, 1996.

Manuscript was received on 15 July 1996, in revised form 15 January 1997.